JOURNAL OF Applied Polymer SCIENCE

Syntheses, Characterization, and Antibacterial Activity of Chitosan Grafted Hydrogels and Associated Mica-Containing Nanocomposite Hydrogels

Supaporn Noppakundilograt,[1] Kittichai Sonjaipanich,[2] Nuttha Thongchul,[3] Suda Kiatkamjornwong[1,4]

[1]Department of Printing and Imaging Technology, Faculty of Science, Chulalongkorn University, Bangkok 10330, Thailand
[2]Program of Petrochemistry and Polymer Science, Faculty of Science, Chulalongkorn University, Bangkok 10330, Thailand
[3]Institute of Biotechnology and Genetic Engineering, Chulalongkorn University, Bangkok 10330, Thailand
[4]Division of Science, the Royal Institute of Thailand, Sanam Seuba, Dusit 10300, Thailand
Correspondence to: S. Kiatkamjornwong (E-mail: ksuda@chula.ac.th)

ABSTRACT: Chitosan (CS) grafted poly[(acrylic acid)-*co*-(2-hydroxyethyl methacrylate)] (CS-*g*-poly(AA-*co*-HEMA)) at different molar ratios of AA and HEMA, and the associated nanocomposite hydrogels of CS-*g*-poly(AA-*co*-HEMA)/mica were synthesized by radical copolymerization. The grafting positions at the amino or hydroxyl groups in the CS were identified by Fourier transform infrared spectroscopy. CS-*g*-poly(AA-*co*-HEMA) hydrogels were intercalated in the mica and the amount of hydrogel insertion did not affect the spacing of the silicate layers in mica. The higher mica loadings produced a rougher surface of the nanocomposite hydrogel. The water absorbency of the CS-*g*-poly(AA-*co*-HEMA)/mica nanocomposite hydrogels decreased with increasing levels of mica loading to a lower level than those of the CS-*g*-poly(AA-*co*-HEMA) hydrogels. Both CS-*g*-poly(AA) and CS-*g*-poly(AA-*co*-HEMA)/mica nanocomposite hydrogels exhibited a higher antiproliferative activity against *Staphylococcus aureus* than did the neat CS hydrogel with CS-*g*-poly(AA) revealing a very pronounced minimum inhibition concentration (MIC) of 1.56 mg mL^{-1}. The extent of mica loading in the CS-*g*-poly(AA-*co*-HEMA) nanocomposite hydrogels did not affect the MIC (12.5 mg mL^{-1}). © 2012 Wiley Periodicals, Inc. J. Appl. Polym. Sci. 000: 000–000, 2012

KEYWORDS: chitosan; acrylic acid; 2-hydroxyethyl methacrylate; mica; nanocomposite hydrogel; antibacterial property; swelling; organoclay; biocompatibility

Received 22 March 2011; accepted 28 February 2012; published online 00 Month 2012
DOI: 10.1002/app.37612

INTRODUCTION

Hydrogels are slightly crosslinked hydrophilic polymers that can swell and absorb water at least 15 times their dry weight. The relative density of hydrophilic groups and the degree of crosslinking of the hydrogel are the two main factors that affect the water absorbency of a hydrogel.[1] Chitosan (CS) has found wide applications because of its interesting biological properties, such as biocompatibility, biodegradability, hemostatic activity, and bacteriostatic effects. The mechanism of antibacterial activity of CS has not yet been fully elucidated. However, the most feasible hypothesis is the interaction between the positively charge of CS and the negatively charge of cell membrane of bacterial leading to a change in the cell membrane permeability and resulting in leakage of proteinaceous and other intracellular constituents. Thus, CS affected the gram-positive bacteria than that of gram-negative bacteria which has an efficient outer permeability membrane against macromolecules, such as, chitosan to reach its cytoplasmic membrane.[2] Derivative of CS, such as Schiff base of CS and acylated CS, also showed antibacterial activity.[3] As mentioned above, CS-based hydrogels have been extensively researched and used in a wide field of applications because of their biocompatibility, biodegradability, nontoxicity, and antibacterial activity,[4] because CS is a plentiful, renewable, and relatively cheap material. The hydrogels derived from CS grafted with hydrophilic vinyl monomers, such as acrylic acid (AA) or itaconic acid (IA), showed an increased water absorbency compared to CS alone.[5–7] The 2-hydroxyethyl methacrylate (HEMA) monomer has long been used in biomedical applications because it improves the graft copolymer biocompatibility.[8] HEMA monomer is harmful in the dental application if it does not completely polymerize, because it induces DNA damage, apoptosis, and cell-cycle delay by the production of reactive

oxygen species. However, it was found that the presence of antioxidant and/or CS can decrease the genotoxicity of HEMA monomer.[9,10] CS-*g*-poly(AA-*co*-HEMA) was reported to exhibit good cytocompatibility and hemocompatibility and thus possesses a high potential as an application for wound dressing.[5] Suitable wound dressings normally possess an antibacterial activity for protecting the wound from infection, and have a water absorbency of around 25 to 32 times its dry weight so as to be able to remove secretion or pus from the wound.[11] Bacterial infection is one of the main factors for the development of chronic wounds. Infected wounds may cause trauma and higher treatment costs. Pathogens frequently associated with wound infections include *Staphylococcus aureus (S. aureus)*, *Enterococcus* sp., *Escherichia coli*, *Pseudomonas aeruginosa*, *Enterobacter* sp., *Proteus mirabilis*, *Klebsiella pneumonia*, *Streptococcus* sp., and *Candida albicans*. *S. aureus* is the most commonly found human pathogens which cause wound infections, boils, pustules and other human skin infections.[12] Infection by *S. aureus* is accounted for about 20% frequency of occurrence in burns, wounds, and surgical sites. Due to the above-mentioned causes, any developed wound dressing materials should therefore possess an inhibitory effect on the most frequently found *S. aureus* in wounds.

Generally, the gel strength of a bio-absorbent is naturally rather weak and this unfortunately limits its useful applications. To improve the gel strength, thermal and inherently antibacterial properties of CS and/or grafted CS, clay minerals, such as montmorillonite,[13] rectorite,[14,15] and sepiolite,[16] have been used as a filler incorporated into the CS to produce CS/nanocomposite hydrogels. Quaternized CS/organic montmorillonite nanocomposites strongly inhibited the growth of gram-positive and gram-negative bacteria.[17] Wang et al.[18] found that the antibacterial activity against *S. aureus* of CS/rectorite nanocomposite film was better than that of the neat CS film. This result agreed with the research reporting that clay minerals alone did not destroy bacteria, but they could adsorb and kill bacteria when the antimicrobial materials were intercalated into silicate layers.[19]

Mica is a clay mineral known as a 2 : 1 phyllosilicate and its general formula is $AM_{2\text{-}3}T_4O_{10}X_2$, where A is usually Na, K, or Ca. The M can be Fe, Al, and Mg; T is Si and/or Al and X is (OH), O, Cl, and F.[20] It is composed of two-dimensional layers of an edge-shared octahedral sheet that is fused to form two tetrahedrals by the shared oxygen ions of one octahedral sheet and two tetrahedral sheets.[21] Mica shows the antimicrobial activity, but it has a tendency of cytotoxicity with a larger platelet size than that of montmorillonite.[22] Nanosilicate platelet of montmorillonite has a low cytotoxicity with antibacterial activity.[22,23] However, only a few research reports on CS/mica nanocomposite hydrogels are available, leaving its potential suitability for many applications, including as a wound dressing material, unknown. Therefore, the synthesis and characterization of grafted CS/mica nanocomposite hydrogels was the main aim of this research. The effects of the reaction parameters on the morphology, water absorption, and antibacterial activities of the resultant hydrogels were investigated.

EXPERIMENTAL

Materials

CS with a viscosity average molecular weight of 57,000 g mol^{-1} and an 85% deacetylation degree was purchased from Seafresh Industry Public Co., Ltd. (Bangkok, Thailand). Industrial grade AA and HEMA monomers were kindly supplied by Thai Mitsui Specialty Chemicals Co., Ltd. (Bangkok, Thailand). *N*,*N*′-methylenebisacrylamide (*N*-MBA) crosslinker and *N*,*N*,*N*′,*N*′-tetramethylethylene diamine (TEMED) co-initiator were purchased from Fluka (Buchs, Switzerland). Ammonium persulphate (APS), purchased from Ajax (Australia), was used as the initiator. Swelling mica was purchased from Wako Pure Chemical Industries, Ltd. (Osaka, Japan). Deionized water, used as the reaction medium, was obtained from an Elga Deionizer (Model LA611, Marlow international, Bucks, UK). Sodium ampicillin (drug grade) was purchased from T.P. Drug Laboratories (Bangkok, Thailand). *S. aureus isolated* from textile wastewater was provided by the National Center for Genetic Engineering and Biotechnology (NSTDA, Pathum thani, Thailand). Mueller-Hinton Broth (MHB) and Mueller-Hinton Agar (MHA), used for the growth of *S. aureus* were from Difco, New Jersey, USA.

Syntheses

Synthesis of Grafted CS Hydrogels. CS (1 g) was added into 30 mL of 2% w v^{-1} acetic acid solution in a 500 mL four-necked round-bottomed flask with a mechanical stirrer (Ika RW 28, IKA® Werke GmbH & Co. KG, Staufen Germany), assembled with a half-moon shaped Teflon blade paddle and a condenser. The mixture was stirred for 30 min at room temperature and then heated at 60 ± 2°C under nitrogen gas which was fed constantly through the gas inlet at 10 mL min^{-1} for 30 min. APS (0.01–0.15 g) was then added and stirred for 10 min, followed by the sequential addition of either AA or HEMA or both and *N*-MBA (0.01–0.15 g) to the desired final concentration and stirred for 5 min. Finally, TEMED was added (0.01–0.4 g) to the mixture and stirred at 250 rpm for another 60 min. The reaction was then cooled down to room temperature and adjusted to pH 8 by 1*M* sodium hydroxide solution. The product was dewatered with acetone, cut into pieces of approximately 1 × 1 cm square and dried in an oven at 50°C for 24 h. The dried product was extracted with an excess amount of methanol in a Soxhlet apparatus for 24 h to remove the unreacted components and obtain the CS grafted polymer (e.g. CS-*g*-poly(AA-*co*-HEMA)). The extracted product was dried in the oven at 50°C for 24 h, milled and sieved through a 100 mesh sieve to obtain the hydrogel particles in the range of 50 to 100 mesh (200–400 μm).

Synthesis of CS-*g*-Poly(AA-co-HEMA)/Mica Nanocomposite Hydrogels. The desired amount of mica was dispersed in the mixture of AA and HEMA monomers for 60 min by stirring at 250 rpm with a magnetic stirrer. CS (1 g) was dissolved in 30 mL of 2% v v^{-1} solution of acetic acid, and then added into a 500 mL four-necked round-bottomed reaction flask equipped with the mechanical stirrer and a condenser. The reactor was then immersed in a temperature controlled water bath, stirred at 250 rpm under a constant nitrogen gas fed through the gas inlet tube for 30 min before APS (0.1 g) was added and stirred for 10 min. The well-dispersed mica suspension was added into

the solution of CS and APS, stirred at 250 rpm and heated to 60 ± 2°C under the nitrogen gas circulation for 30 min before *N*-MBA (0.1 g) was then added and stirred for 5 min. Finally, TEMED (0.4 g) was added and stirred for another 60 min. The polymerization product was cooled down and the product was obtained by the same procedure as described above for the grafted CS hydrogels.

Grafting Ratio and Efficiency of the Grafted CS Hydrogels by Acid Hydrolysis. The grafted CS hydrogel (0.5 g) was dissolved in 50 mL of 1*M* HCl in a 125 mL Erlenmeyer flask which was assembled with a condenser and refluxed at 120°C for 2 h. After the acid hydrolysis, the remaining solid (grafted copolymer) was filtered, dried, and weighed. The filtrate was neutralized to pH 7 by 1*M* sodium hydroxide solution and then precipitated by ethanol. The precipitate was filtered and dried at room temperature for 24 h to obtain its dry weight. Finally, the filtrate from the precipitation step was evaporated to remove the residual solvent. The white solid was dried at room temperature and weighed. The remaining solid and precipitate after the acid hydrolysis were investigated for functional groups by Fourier transform infrared spectroscopy (FTIR; model Tensor 27, Billerica) using KBr pellets. The grafting ratio, grafting efficiency, and homopolymer content were calculated from eqs. (1)–(3)[24–26]:

$$\%\ \text{Grafting efficiency} = \text{Weight of remaining solid after acid hydrolysis} \times 100/\text{weight of homopolymer} + \text{weight of grafted copolymer} \quad (1)$$

$$\%\ \text{Grafting ratio} = \text{Weight of remaining solid after acid hydrolysis} \times 100/\text{weight of precipitate fromethanol} \quad (2)$$

$$\%\ \text{Homopolymer} = \text{Weight of grafted CS hydrogel before Soxhlet extraction} - \text{weight of grafted CS hydrogel after Soxhlet extraction} \quad (3)$$

Identification of Functional Groups of Grafted CS Hydrogels and CS-*g*-Poly(AA-*co*-HEMA)/Mica Nanocomposite Hydrogels. The functional groups of mica, the grafted CS hydrogels and grafted CS-*g*-poly(AA-*co*-HEMA)/mica nanocomposite hydrogels were characterized by FTIR with 32 scans and 4 cm^{-1} resolution.

Characterization of the Grafted CS Hydrogels and CS-*g*-Poly (AA-*co*-HEMA)/Mica Nanocomposite Hydrogels. The surface morphologies of the mica, and the grafted CS and grafted CS/mica nanocomposite hydrogels were photographed on a scanning electron microscope (SEM, model JSM-5410LV, Tokyo, Japan) without prior cross sectioning. Each sample was fixed on an aluminum stub and coated with gold. X-ray diffraction (XRD) patterns of the samples were recorded using Bruker AXS (model D8 Discover, Bruker AXS Munich, Germany) with Cu radiation, voltage of 40 kV, a current of 40 mA and scanned from 1 to 35° with a scanning rate of 0.02° min^{-1}. The transmission electron micrographs (TEM) were taken on JOEL (JEM-2100, Jeol Ltd., Tokyo, Japan).

The Effect of the Reagent Contents on Water Absorbency of Grafted CS Hydrogels and CS-*g*-Poly(AA-*co*-HEMA)/Mica Nanocomposite Hydrogels. The water absorbencies of the grafted CS hydrogel and the grafted CS-*g*-poly(AA-*co*-HEMA)/mica nanocomposite hydrogels were carried out with distilled water at room temperature in a closed system to minimize water evaporation. Distilled water (200 mL) was added to 0.1 g of the dry grafted hydrogels or the nanocomposite hydrogels. The hydrogel was swollen to equilibrium for 24 h and the swollen gel was then filtered through a 100-mesh aluminum screen sieve for 2 h. The water absorbency was determined for at least three replications for each synthesized product by eq. (4):

$$\text{Water absorbancy}(Q) = (W_s - W_d)/W_d \quad (4)$$

where W_s is the weight of swollen hydrogels or nanocomposite hydrogels (g) and W_d is the weight of the dry hydrogels or nanocomposite hydrogels (g).

Absorbency Under Load (AUL). The dry hydrogel weighing 0.1 g was put on the 100-mesh aluminum screen sieve assembled with an aluminum cylinder (26 mm in diameter and 35 mm in height) and was then immersed in 50 mL of distilled water in a Petri dish. The load of 0.7 psi (4.833×10^3 Pa), was placed on the top of dry CS-*g*-poly(AA-*co*-HEMA) hydrogel or CS-*g*-poly(AA-*co*-HEMA)/mica nanocomposite hydrogel. After 1 h swelling under load, the water absorbency of CS-*g*-poly(AA-*co*-HEMA) hydrogel or CS-*g*-poly(AA-*co*-HEMA)/mica nanocomposite hydrogel was calculated from eq. (4) and reported as an average with one standard deviation. The water absorbency of CS-*g*-poly(AA-*co*-HEMA) hydrogel or CS-*g*-poly(AA-*co*-HEMA)/mica nanocomposite hydrogel without load (unloaded) was measured with the same procedure.

Antibacterial Activity

Turbidity Method. The CS, CS-*g*-poly(AA), CS-*g*-poly(HEMA) and CS-*g*-poly(AA-*co*-HEMA) hydrogels, and the CS-*g*-poly(AA-*co*-HEMA)/mica nanocomposite hydrogels, each weighing 250 mg, and distilled water were sterilized by UV radiation for 1 h before the test.

The diluted stock culture of *S. aureus* was adjusted to 0.5 units by sterile deionized water. The *S. aureus* suspension (2.5 mL) was inoculated into 47.5 mL of sterile Mueller-Hinton Broth (MHB) in a 250 mL sterile Erlenmeyer flask. For each hydrogel type, the sterile sample (250 mg) was then added to the *S. aureus* suspension in MHB media and incubated at 37°C while being shaken at 250 rpm. At every 2 h a 50-mL aliquot was harvested and the swollen gel was removed by filtration through filter paper no. 1 (Schleicher & Schuell, Whatman, Kent, UK) before measuring the $OD_{610\ nm}$ of the filtrate as a measure of the growth of *S. aureus* using a spectrophotometer (Spectronic 21, Bausch & Lomb Inc., Rochester, NY). Two replicate experimental points at 6 and 8 h of the growth curve were carried out to observe its variation. The OD results of the growth with or without the hydrogel were plotted versus time to obtain the bacterial growth profiles. The culture time at which the antibacterial activity of the grafted CS hydrogel was found to be maximal by the optical density measurement was used to evaluate the total replication competent (viable) bacterial number using the total plate count method (see Total plate count method section below) so as to calculate the mean colony-

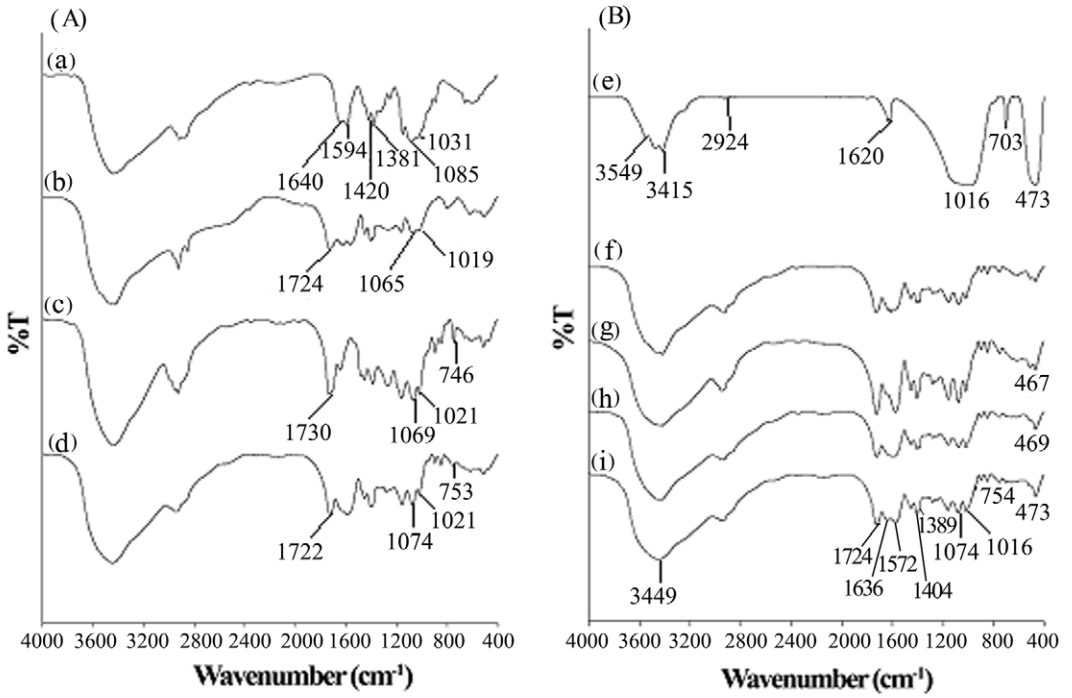

Figure 1. Representative FTIR spectra of (A): (a) CS, and (b) CS-*g*-poly(AA), (c) CS-*g*-poly(HEMA), and (d) CS-*g*-poly(AA-*co*-HEMA) hydrogels, the last being synthesized with an AA: HEMA, N-MBA : CS, APS : CS, and TEMED : CS molar ratios of 1, 0.11, 0.07, and 0.58, respectively; the spectra (B): (e) mica, and CS-*g*-poly(AA-*co*-HEMA)/mica nanocomposite hydrogels with mica loadings of: (f) 5%, (g) 7%, (h) 10%, and (i) 15% w w^{-1} based on the monomer.

forming units per milliliter (CFU mL^{-1}), and from this the relative degree of inhibition of bacterial proliferation can be obtained.

Total Plate Count Method. The 6- and 8-h-old *S. aureus* cultures in MHB were diluted with sterile deionized water to 10^8 to 10^9 CFU mL^{-1} and then 100 μL aliquots of each diluted *S. aureus* suspension were spread on each MHB plate. The plates were incubated for 24 h at 37°C whereupon the number of viable bacteria was counted. Mean CFU mL^{-1} and the relative inhibition were calculated by eqs. (5) and (6), respectively. The negative control was the sterilized *S. aureus* cultured in MHB.

$$\text{CFU/mL} = (\text{Mean numbers of counted colonies/amount of diluted } S.\ aureus \text{ for spread plate (mL)} \times \text{dilution factor} \quad (5)$$

$$\text{Relative inhibition} = 100 - (\text{CFU/mL of the sample/CFU/mL of negative control}) \times 100 \quad (6)$$

Minimum Inhibition Concentration (MIC). The antibacterial activity was determined in terms of the minimum inhibition concentration (MIC). The diluted stock culture of *S. aureus* was adjusted to 0.5 A_{610} units by sterile deionized water and 100 μL was inoculated into 4.9 mL of sterile MHB in a 10 mL test tube. The hydrogels, each evaluated at the five concentrations of 0, 3.12, 6.25, 12.5, and 25 mg mL^{-1}, were added to the 0.01 A_{610} unit suspensions of *S. aureus* (see above) in the sterile MHB. The cultures were then incubated at 37°C while shaking at 120 rpm for 24 h. The mean CFU mL^{-1} of each sample tested was measured by the total plate count method as above and the experiment was performed in triplicate. The MIC was thus determined from the derived CFU mL^{-1} and statistical significance (ANOVA) was accepted at the 99% significant level or $\alpha = 0.01$.

RESULTS AND DISCUSSION

Characterization of the Grafted Hydrogels

Grafted CS Hydrogels. The spectrum of the CS hydrogel [Figure 1(a)] shows the characteristic amino group peaks at 3428 cm^{-1} for N-H stretching, 1640 cm^{-1} for the C=O stretching of amide I,[27] 1594 cm^{-1} for the N—H bending of amide II, 1381 cm^{-1} for the —NHCO stretching of amide II[28], and 1253 cm^{-1} for C—N stretching.[29] The characteristic peaks of the saccharide structure in CS exhibit at 1152 cm^{-1} for the bridge O stretching,[26,30] and 1085 cm^{-1} and 1031 cm^{-1} for the C_3-OH and C_6-OH stretching, respectively.[28] In addition, the absorption peak at 1420 cm^{-1} is the O-H and C-H vibration which indicates the presence of a hydroxyl group.[27] The peak of C-H stretching appears at 2921 and 2864 cm^{-1}.[30]

The CS-*g*-poly(AA) hydrogel spectrum [Figure 1(b)] shows a new absorption peak at 1724 cm^{-1} assigned to C=O stretching of the carboxyl group from the grafted poly(AA) part,[30] which was shifted from the peak at 1713 cm^{-1} of the carboxyl group of poly(AA). In addition, the new absorption peaks at 1563 cm^{-1} and 1402 cm^{-1} are ascribed to asymmetric and symmetric stretching of the carboxylate anion of poly(AA) in the CS-*g*-poly(AA) hydrogel.[5] The absorption peak at 1594 cm^{-1}, assigned to N—H bending of CS, disappeared in the CS-*g*-poly (AA) hydrogel. Thus, the NH_2 group is grafted in the CS

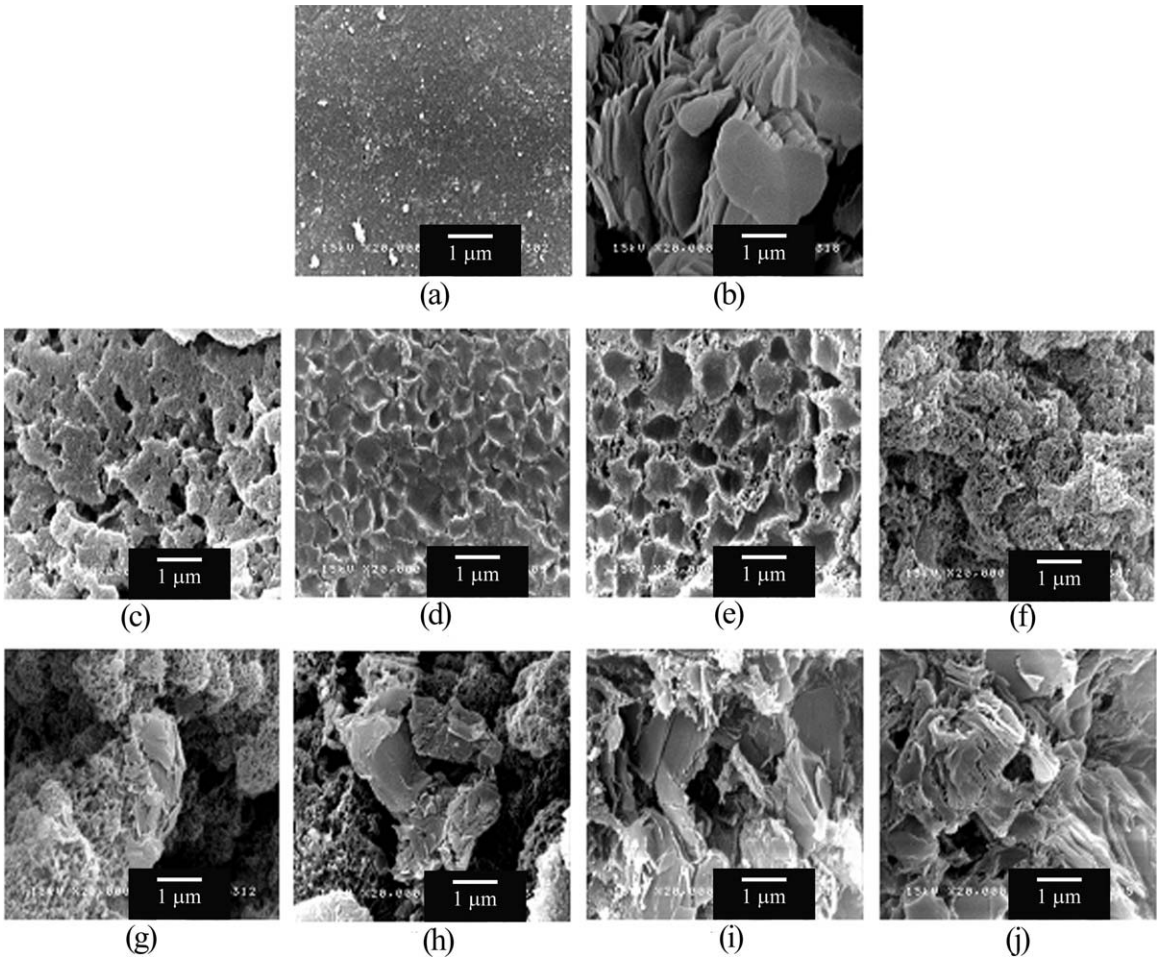

Figure 2. Representative SEM micrographs of (a) CS, (b) mica, (c) CS-*g*-poly(AA), (d) CS-*g*-poly(HEMA), (e, f) CS-*g*-poly(AA-*co*-HEMA), and CS-*g*-poly(AA-*co*-HEMA)/mica nanocomposite hydrogels synthesized with mica loading levels of (g) 5%, (h) 7%, (i) 10%, and (j) 15% w w^{-1} of the monomer.

backbone.[31] Moreover, the characteristic peaks of the saccharide structure of CS in the CS-*g*-poly(AA) hydrogel was shifted to 1065 cm^{-1} and 1019 cm^{-1} (C_3-OH and C_6-OH stretching) and the peak of O—H bending at 1420 cm^{-1} disappeared [Figure 1(b)]. From these results, the poly(AA) chains were confirmed to be grafted at both the NH_2 and OH sites on the CS backbone.

The CS-*g*-poly(HEMA) spectrum [Figure 1(c)] shows an absorption peak at 1730 cm^{-1}, assigned to C=O asymmetric stretching, which indicates the presence of the ester carbonyl group of poly(HEMA),[5] and a new absorption peak at 746 cm^{-1} that is attributed to the CH_2 rocking of the poly (HEMA) moiety.[32] The absorption peak of N—H stretching of CS also disappeared. Thus, the NH_2 group of CS had been reacted in the graft polymerization.[31] The characteristic peaks of the saccharide structure of CS in the CS-*g*-poly(HEMA) hydrogel were shifted to 1069 cm^{-1} and 1021 cm^{-1} (C_3-OH and C_6-OH stretching) and the CS O—H bending peak at 1420 cm^{-1} [Figure 1(a)] disappeared. Thus, the poly(HEMA) was grafted at both NH_2 and OH sites on the CS backbone as well.

The CS-*g*-poly(AA-*co*-HEMA) hydrogel spectrum [Figure 1(d)] shows the absorption peak at 1722 cm^{-1} that is assigned to the C=O asymmetric stretching and so indicates the presence of the ester carbonyl group of the poly(HEMA) moiety,[5] and a new absorption peak at 753 cm^{-1} that is attributed to the CH_2 rocking of the poly(HEMA) moiety.[32] In addition, it also shows peaks at 1585 cm^{-1} (C=O asymmetric stretching) and 1402 cm^{-1} (C=O symmetric stretching) of the carboxylate anion in the poly(AA) moiety.[5] Moreover, the characteristic peaks of the saccharide structure of CS in the CS-*g*-poly(AA-*co*-HEMA) hydrogel [Figure 1(d)] shifted to 1074 and 1021 cm^{-1} (C_3-OH and C_6-OH stretching) and the peak of O—H bending at 1420 cm^{-1} [Figure 1(a)] disappeared [Figure 1(d)]. Thus, poly(AA-*co*-HEMA) was also grafted at both the NH_2 and OH sites on the CS backbone.

CS-*g*-poly(AA-*co*-HEMA)/Mica Nanocomposite Hydrogels. The FTIR spectrum of mica is shown in Figure 1(e). It shows a peak of O—H stretching at 3600 to 3400 cm^{-1} that indicates the presence of the hydroxyl group. The absorption peaks at 2924 and 2852 cm^{-1} are attributed to the C—H stretching of the organic part and indicate that the mica used is a synthetic one. It

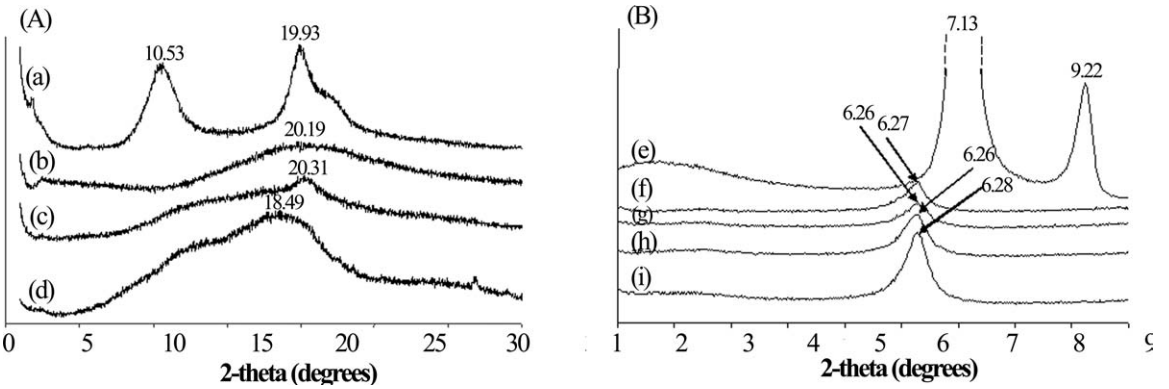

Figure 3. Representative XRD patterns of hydrogels synthesized from (A): (a) CS, (b) CS-*g*-poly(AA) synthesized with 1 g CS, 54 mmol AA, and N-MBA, APS and TEMED at 10%, 10%, and 40% w w^{-1} of CS, respectively, (c) CS-*g*-poly(AA-*co*-HEMA) and (d) CS-*g*-poly(HEMA); (B): (e) mica, and CS-*g*-poly(AA-*co*-HEMA)/mica nanocomposite hydrogels synthesized with mica loadings of (f) 5%, (g) 7%, (h) 10%, and (i) 15% w w^{-1} based on the monomer, 1 g CS, an AA : HEMA molar ratio of 1 : 1, and N-MBA, APS and TEMED at 10%, 10%, and 40% w w^{-1} of CS, respectively.

also shows the absorption peaks of H—O—H bending of water at 1637 and 1620 cm^{-1},[33] and Si—O and Al—O stretching peaks at 1016 and 473 cm^{-1}.[34]

The FTIR spectra of CS-*g*-poly(AA-*co*-HEMA)/mica nanocomposite hydrogels, containing mica at 7, 10, or 15% w w^{-1} of the monomer, are shown in Figure 1(f–h), respectively. In comparison with the spectra of mica [Figure 1(e)], the characteristic peaks of CS are shifted to 1636 and 1389 cm^{-1}, whilst the characteristic peaks of poly(AA-*co*-HEMA) are also shifted to 1724, 1572, 1404, and 754 cm^{-1}. In addition, new absorption peaks appear at 473, 469, and 467 cm^{-1} [Figure 1(f–h), respectively], all of which are attributed to the Al—O stretching of mica. The intensity of the absorption peak at 1016 cm^{-1} (Si—O stretching) increased with increasing mica loadings in the CS-*g*-poly(AA-*co*-HEMA)/mica nanocomposite hydrogels, which indicates the existence of mica in the CS-*g*-poly(AA-*co*-HEMA) nanocomposite hydrogel. Based on these FTIR data, the AA or HEMA group is grafted at the OH group of the C-6 position and/or the amino group of CS. The FTIR peaks in the spectra further confirmed that CS-*g*-poly(AA-*co*-HEMA)/mica nanocomposite hydrogels with various loadings of mica were successfully synthesized.

The Grafting Performance of Grafted CS Hydrogels

Analysis of the acid hydrolysis suggests the grafting ratio of the CS-*g*-poly(AA) hydrogel (87%) is lower than that of the CS-*g*-poly(AA-*co*-HEMA) (269%) and CS-*g*-poly(HEMA) hydrogels (343%). However, the grafting ratios of CS-*g*-poly(AA-*co*-HEMA) and CS-*g*-poly(HEMA) hydrogels were calculated from the weight differences because a poly(HEMA) C=O peak at 1710 and 1722 cm^{-1} is still observed. Thus, at least some poly(HEMA) is still incorporated in the precipitate after acid hydrolysis, it means that the acid hydrolysis of the CS-*g*-poly(HEMA) was not completed. In comparison with the amount of CS, a greater amount of HEMA was used and so HEMA can generate an interpenetrate polymer network (IPN) hydrogel[35] on the CS backbone. This result reflects the high grafting ratio as expected. The grafting efficiency of CS-*g*-poly(AA), CS-*g*-poly(AA-*co*-HEMA), and CS-*g*-poly(HEMA) hydrogels is 93, 94, and 96%, respectively. The amount of homopolymer normally generated during graft polymerization and the homopolymer chains could form the IPN chains. Therefore, the amount of homopolymer cannot be derived directly just from the Soxhlet extraction and acid hydrolysis. Therefore, the amounts of free poly(AA), poly(AA-*co*-HEMA), and poly(HEMA) found are only 3, 5, and 3%, respectively, which are considered to be quite small, and would probably have been incorporated as the IPN in the polymeric hydrogels.

Surface Morphology

The surface morphologies of the CS, mica, CS-*g*-poly(AA-*co*-HEMA) hydrogel, and CS-*g*-poly(AA-*co*-HEMA)/mica nanocomposite hydrogels with 5 to 15% (w w^{-1} of the monomer) mica loadings are shown as the representative SEM micrographs

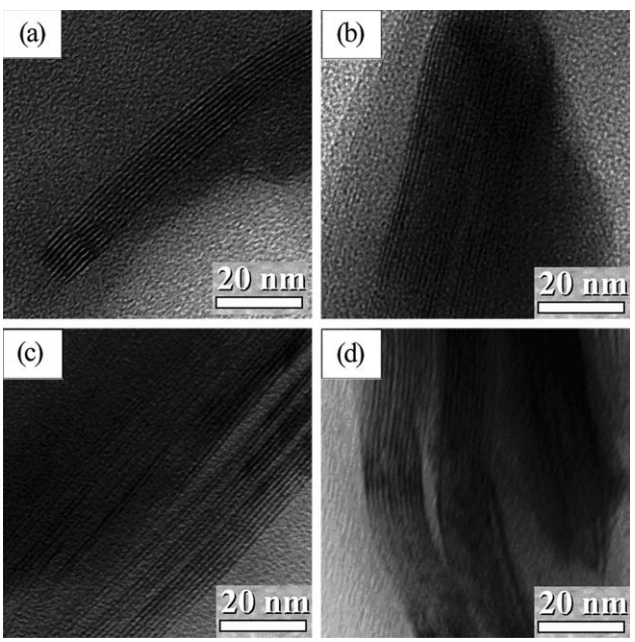

Figure 4. Representative TEM micrographs of CS-*g*-poly(AA-*co*-HEMA)/mica composite hydrogels synthesized with mica loadings of (a) 5%, (b) 7%, (c) 10%, and (d) 15% w w^{-1} based on the monomer.

Table I. The Water Absorbency of Hydrogels Derived from CS, AA and /or HEMA Grafted-CS Copolymers and CS-*g*-poly(AA-*co*-HEMA)/Mica Nanocomposites

Polymer	AA : HEMA (mol ratio)	Mica (w w^{-1} of monomer)	Water absorbency (g g^{-1})[a]
CS	-	--	10 ± 2
CS-*g*-poly(AA)	--	--	101 ± 4
CS-*g*-poly(HEMA)	--	--	11 ± 1
CS-*g*-poly (AA-*co*-HEMA)	3 : 1	--	64 ± 2
	1 : 3	--	20 ± 2
	1 : 1	--	54 ± 3
	1 : 1	5	45 ± 3
	1 : 1	7	44 ± 1
	1 : 1	10	46 ± 2
	1 : 1	15	35 ± 5

[a]Data are shown as the mean ± 1 SD and are derived from five repeats. Means within the column are significantly different ($P < 0.05$).

in Figure 2. The relatively smooth surface of the CS hydrogel and the flat sheets of mica at approximately 1 to 3 μm along with their aggregated state is clearly visible [Figure 2(a,b)]. The surface of the CS-*g*-poly(AA) hydrogel [see Figure 2(c)] exhibits the larger porous structure in many areas than those of CS-*g*-poly(HEMA) [see Figure 2(d)] and CS-*g*-poly(AA-*co*-HEMA) hydrogel [see Figure 2(e,f)]. The surface morphology of the CS-*g*-poly(HEMA) hydrogel shows a gel network surrounded by a wide spread of uniformly distributed micropores and this is especially regular on the surface of the CS-*g*-poly(AA-*co*-HEMA) hydrogel [Figure 2(d)]. The CS-*g*-poly(AA-*co*-HEMA) hydrogel surface exhibits further a nanoporous structure [Figure 2(e,f)].

The internal morphologies of the CS-*g*-poly(AA-*co*-HEMA)/mica nanocomposites containing 5 to 15% w w^{-1} mica of the monomer [Figure 2(g–j)] are slightly different from those of the mica-free CS-*g*-poly(AA-*co*-HEMA). It is seen that the higher the mica loading, the more the surface roughness increased and that the mica flakes are imbibed in the inner areas of the gel. When the mica loadings were too high, they were aggregated, agglomerated, resided, deposited, and covered the whole polymer surface. Based on these results, CS-*g*-poly(AA-*co*-HEMA)/mica nanocomposite hydrogels are confirmed to have been successfully synthesized. One must state that no residual HEMA was retained in the resulting hydrogels because no indication of the double bonds peaks was found in the IR spectra because many extractions of the unused materials were made in solvent.

XRD and TEM Analyses

The XRD pattern of the CS hydrogel [Figure 3(a)] shows the 2-theta of CS at 10.53° and 19.93°, which corresponds to the hydrated crystals of low crystallinity of the form I and crystallinity of the form II, respectively.[36,37] The XRD pattern of CS-*g*-poly(AA), CS-*g*-poly(HEMA), and CS-*g*-poly(AA-*co*-HEMA) exhibit the broader and weaker peaks at 20.19, 18.49, and 20.31°, respectively, whereas the 2-theta at 10.53° of all these three CS grafted hydrogels disappeared. These indicated that the crystallinity of the grafted CS was dramatically decreased. Changes in the intensity of the peaks at approximately 20° relate to different packing of the chains and/or different hydrogen bonding networks in the grafted CS.[38] Thus, the introduction of AA and/or HEMA chains onto the surface of the CS causes the breakdown of its crystallinity. These results confirmed that the grafting of polymer onto the CS chain occurred.[36,37,39] The XRD patterns of mica revealed 2-theta values of 7.13 and 9.22° that correspond to a basal spacing of 13.58 and 9.58 Å, respectively. The XRD patterns of the CS-*g*-poly(AA-*co*-HEMA)/mica nanocomposite hydrogel reveal that the 2-theta value of mica in the nanocomposite hydrogels were shifted toward a lower angle (6.27°) and that the interlayer spacing of mica increased by 1.7 Å compared with that of the swelling mica. This confirms that intercalation had taken place and that the CS-*g*-poly(AA-*co*-HEMA)/mica nanocomposite hydrogels are intercalated composites with more spacing in the silicate layers.[40] In addition, it also shows that increasing the mica loadings from 5 to 15% (w w^{-1} based on the weight of monomer) does not affect the intercalated structure of the CS-*g*-poly(AA-*co*-HEMA)/mica nanocomposite hydrogels but rather they exhibit the same basal spacing. These results agree well with the previous report of Wang et al.[14]

Representative TEM micrographs of the CS-*g*-poly(AA-*co*-HEMA)/mica nanocomposite hydrogels with mica loadings of 5, 7, 10, and 15% w w^{-1} of the monomer are shown in Figure 4. The dark lines in Figure 4 belong to the mica structure and the bright area is the grafted chitosan matrix. All the TEM micrographs of nanocomposite hydrogels revealed that the distance between the two adjacent dark lines, the spacing of the two silicate layers, results in an intercalated structure. Indeed, parts of the silicate layer can be seen in Figure 4(a–d). The results of the TEM analysis are consistent with the XRD data (Figure 3), and support that CS-*g*-poly(AA-*co*-HEMA)/mica nanocomposite hydrogels have an intercalated structure and no significance at any level of an exfoliated structure is observed.

Equilibrium Water Absorbency

Effect of Monomer Type (AA or HEMA) on the Properties of the Grafted CS Hydrogels. The equilibrium water absorbency of CS alone was rather low but was significantly affected by the

Table II. Effect of Mica Loading on Water Absorbencies at Unloaded and Loaded with 0.7 psi of CS-*g*-poly(AA-*co*-HEMA)/Mica Nanocomposite Hydrogel

CS-*g*-poly(AA-*co*-HEMA) hydrogel with mica loading (%)	Water absorbency (g g^{-1})[a]		
	Unload	Under load (0.70 psi)	Unload/ under load (fold)
0	39 ± 2	16 ± 1	2.4
5	32 ± 0	18 ± 1	1.8
7	31 ± 1	18 ± 1	1.7
10	30 ± 0	19 ± 1	1.6
15	21 ± 1	17 ± 1	1.2

[a]The water absorbency was determined in triplicate.

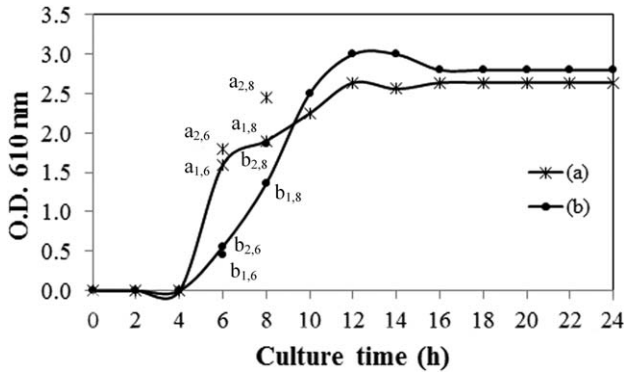

Figure 5. The optical density at 610 nm of *S. aureus* cultured in HMB media at various culture times with (a) the negative control, or 250 mg mL^{-1} of (b) CS-*g*-poly(AA-*co*-HEMA) hydrogel prepared with 1 g CS, an AA : HEMA molar ratio of 1 : 1, and N-MBA, APS, and TEMED at 10%, 10%, and 40% w w^{-1} of CS, respectively, with polymerization performed at 250 rpm and 60°C for 60 min.

copolymerization with AA, but not with HEMA (Table I). CS-*g*-poly(AA) had 10-fold higher water absorbency, whereas the water absorbency of the CS-*g*-poly(HEMA) was not significantly different to that for CS alone (Table I). The water absorbency of the CS-*g*-poly(AA-*co*-HEMA) decreased ~ 1.2- and 3.2-fold as the AA : HEMA ratios decreased from 3 : 1 to 1 : 1 and 1 : 3, respectively (Table I). That the water absorbency of CS-*g*-poly(AA-*co*-HEMA) increased as the content of AA increased is due to the increase in the density of hydrophilic groups from the carboxylic acid contents,[41] which then provides a greater repulsion of the anionic portion allowing for the expansion of the polymer chains. This also then explains the increased water absorbency of the CS-*g*-poly(AA) hydrogels over that of the CS hydrogels. On the other hand, CS-*g*-poly(HEMA) had very low water absorbency because HEMA is not as polar as AA but rather has a rather rigid chain due to the methacrylate substituent group. The longer chain of the poly(HEMA) hydrogel thus is likely to have resulted in more molecular entanglements that limited the chain expansion[42] and caused the water absorbency of the CS-*g*-poly(HEMA) hydrogel to decrease. Thus, although CS-*g*-poly(HEMA) would be unlikely to be beneficial to intercalate with mica, the HEMA moiety is more compatible with human cells than the other types of monomer moieties.

Effect of Mica Loading. The equilibrium water absorbency of the CS-*g*-poly(AA-*co*-HEMA) hydrogel at a 1 : 1 AA : HEMA molar ratio was ~ 5.4- and 5-fold higher than that of CS or CS-*g*-poly(HEMA), respectively, but almost half that of the CS-*g*-poly(AA) hydrogel (Table I). The addition of mica at 5, 7, or 10% (w w^{-1} of monomer) caused a 1.2-fold drop in the equilibrium water absorbency from that seen with the mica-free CS-*g*-poly(AA-*co*-HEMA) hydrogel, but did not vary significantly between the three different mica loading levels (Table I). In contrast, when the mica loading was increased to 15% w w^{-1} of monomer, the water absorbency was significantly decreased a further 1.3-fold compared with that seen with the 5 to 10% w w^{-1} mica loaded CS-*g*-poly(AA-*co*-HEMA), or 1.54-fold less than that for the mica-free CS-*g*-poly(AA-*co*-HEMA). This is because the polymer chains were inserted into the spacing between the silicate layers of mica and so the polymer chains were restricted in these limited spaces and so less able to expand. Another reason could be the degree of rigidity of the nanocomposite hydrogel that is induced by the mica. This also supports the notion that the structure of this nanocomposite hydrogel was intercalated.

The water absorbency under load (WAUL) can be indirectly used to determine the gel strength of hydrogel. The higher AUL value, the greater the gel strength of hydrogel becomes. When CS-*g*-poly(AA-*co*-HEMA) hydrogel and CS-*g*-poly(AA-*co*-HEMA)/mica nanocomposite hydrogels absorbed water under a load at 0.70 psi (4.83×10^3 Pa), the water absorbency under load decreases from the unloaded absorbency because the absorbed water in hydrogel was removed by the loading external pressure.[43] The decreasing WAUL of CS-*g*-poly(AA-*co*-

Table III. Total Plate Counts (Replication Competent Cells) and the Relative Inhibition of Growth of *S. aureus* in the Presence of Sodium Ampicillin and the Hydrogels of CS, AA, and/or HEMA Grafted-CS Copolymers and CS-*g*-poly(AA-*co*-HEMA)/Mica Nanocomposites with Various Mica Loadings

		6-h Culture time		8-h Culture time	
Sample type	Mica (% w w^{-1})	CFU mL^{-1} ($\times 10^9$)[a]	Relative inhibition (%)	CFU mL^{-1} ($\times 10^9$)[a]	Relative inhibition (%)
Negative control[b]	--	6.95 ± 1.51	--	8.15 ± 1.25	--
Positive control[c]	--	0	100	0	100
CS[d]	--	2.7 ± 0.25	61	6.4 ± 1.68	21
CS-*g*-poly(AA)[d]	--	0.52 ± 0.48	93	0.91 ± 0.85	89
CS-*g*-poly(HEMA)[d]	--	2.18 ± 0.28	69	5.95 ± 1.25	27
CS-g-poly(AA-*co*-HEMA)[d]	--	1.90 ± 0.19	73	2.92 ± 0.07	64
CS-*g*-poly(AA-*co*-HEMA)[d]	7	1.4 ± 0.37	81	3.6 ± 0.55	57
CS-*g*-poly(AA-*co*-HEMA)[d]	10	1.5 ± 0.34	81	3.9 ± 0.31	54
CS-*g*-poly(AA-*co*-HEMA)[d]	15	5.0 ± 1.68	36	5.9 ± 2.4	30

[a]CFU mL^{-1} is shown as the mean ± 1 SD and are derived from six repeats. Means within a column or across a row are significantly different ($P < 0.05$), [b]Negative control contains only the MHB medium and *S. aureus*, [c]Positive control contains 250 mg of the sodium ampicillin, MHB medium, and *S. aureus*, [d]All hydrogel samples were cocultured with *S. aureus* in MHB media at 250 mg mL^{-1}.

Table IV. Minimum Inhibition Concentration of Hydrogels Derived from CS, AA and/or HEMA Grafted-CS Copolymers and CS-*g*-poly(AA-*co*-HEMA)/Mica Nanocomposites with Various Mica Loadings

Sample	Mica (% w w^{-1})	CFU mL^{-1} ($\times 10^8$)[a]	MIC (mg mL^{-1})[b]
Negative control[c]	--	18 ± 1.0	--
CS[d]	--	10 ± 0.6	25
CS-*g*-poly(AA)[d]	--	3.0 ± 0.4	1.56
CS-*g*-poly(HEMA)[d]	--	6.6 ± 3.5	> 25
CS-*g*-poly(AA-*co*-HEMA)[d]	--	1.2 ± 0.5	12.5
CS-*g*-poly(AA-*co*-HEMA)[d]	5	1.1 ± 0.4	12.5
CS-*g*-poly(AA-*co*-HEMA)[d]	7	5.1 ± 0.6	12.5
CS-*g*-poly(AA-*co*-HEMA)[d]	10	4.6 ± 0.4	12.5
CS-*g*-poly(AA-*co*-HEMA)[d]	15	4.9 ± 4.9	12.5

[a]CFU mL^{-1} is shown as the mean ± 1 SD and is derived from three repeats. Means within the column are significantly different ($P < 0.05$), [b]MIC are shown as mg mL^{-1} for a 2% (v v^{-1}) seeding of a late log phase culture of *S. aureus* in MHB media and evaluated at late stationary phase (24 h of culture), [c]Negative control contains only the MHB medium and *S. aureus*, [d]All hydrogel samples were cocultured with *S. aureus* in MHB media at 250 mg mL^{-1}.

HEMA) hydrogel as seen in Table II is more than those of CS-*g*-poly(AA-*co*-HEMA)/mica nanocomposites because the intercalated structure of these nanocomposites improved the strength of the polymer matrix to absorb more water under load. At 15% w w^{-1} mica loaded CS-*g*-poly(AA-*co*-HEMA), the water absorbency at under load decreased by 1.2-fold compared with unloaded one. WAUL of CS-*g*-poly(AA-*co*-HEMA)/mica nanocomposites decreased with increasing mica loading. Thus, the gel strength of hydrogel/mica nanocomposite increased with more mica loadings.

Antibacterial Activity

Particle sizes of the CS, CS-*g*-poly(AA-*co*-HEMA) hydrogels, and CS-*g*-poly(AA-*co*-HEMA)/mica nanocomposite hydrogel were in the range of 200 to 400 μm classified by the sieve size of 50 to 100 mesh which is anticipated to have an important effect on the bacterial growth inhibition.[44] This was therefore evaluated using a co-culture of *S. aureus* with each hydrogel type and evaluating the bacterial growth relative to the control culture by measuring the culture turbidity by absorbance (after removal of the hydrogel by filtration), and by total plate counts of replication competent ("viable") cells, over a 24-h time period.

Turbidity Method. The well-used method assumes that the turbidity of a medium solution increases solely due to the increase in the number of bacterial cells. Although this method is easy to perform the bacteria sample must be in a liquid suspension state, and typically it can only be used to detect bacteria in the range of 10^6 to 10^7 bacteria mL^{-1}. Moreover, the measurement of bacterial growth in the lag phase is less accurate and is an indirect measurement that needs a calibration curve, where a direct measurement of bacterial counts must be performed.

The preliminary results of the antibacterial activity testing of the CS-*g*-poly(AA-*co*-HEMA) hydrogel, evaluated by measuring the optical density at 610 nm every 2 h and compared with the negative control (containing only the medium and the gram-positive *S. aureus*), revealed three phases in the growth cycle (Figure 5). The lag phases of *S. aureus* growth in the negative control and in the presence of CS-*g*-poly(AA-*co*-HEMA) hydrogel were similar, lasting for 4 h. Then, during the exponential phase, the growth rate of *S. aureus* grown in MHB containing the CS-*g*-poly(AA-*co*-HEMA) hydrogel was lower than that of the negative control during the first 4 h of growth (4–8 h of total culture time). The two replicate data points at 6 and 8 h of culture time as shown in Figure 5 gave the similar trend ($a_{1,6}$ vs. $a_{2,6}$; $a_{1,8}$ vs. $a_{2,8}$ and $b_{1,6}$ vs. $b_{2,6}$; $b_{1,8}$ vs. $b_{2,8}$), therefore, their variation is acceptable. Then this growth rate decreased in the control culture from after 8 h up to reaching the start of the stationary phase (12 h), whereas the growth rate did not slow down in the cultures with CS-*g*-poly(AA-*co*-HEMA) until 10 to 12 h of total culture time, by which time the total bacterial number (as culture optical density) was slightly higher (1.5-fold) than in the control culture. From 12 to 24 h of total culture time, *S. aureus* in both conditions remained in the stationary phase. Thus, the presence of the CS-*g*-poly(AA-*co*-HEMA) hydrogel appeared to render a slower early exponential growth rate of *S. aureus* (or to delay it) but did not reduce the final bacterial density reached after 12 to 24 h in the stationary phase. Since we did not count the viable bacteria that are attached to the gel, or wash them out from the gel, then the CS-grafted hydrogels may not be inhibitory at all but rather the bacteria grow attached to the gel surface and so are not in suspension first and only in suspension subsequently after the gel surface is full swollen and thus has the apparent delayed kinetics.

The Total Plate Count Method. The antibacterial activities of sterile sodium ampicillin (positive control), CS, and grafted CS hydrogels against *S. aureus* were determined by the total plate count method. The mean CFU mL^{-1} and the relative inhibition of CS and grafted CS hydrogels are summarized in Table II. The relative inhibition observed with the CS hydrogel was 2.9-fold greater at 6 h of culture time (early log phase) than that after 8 h of culture (the late log phase). When the CS was grafted with poly(AA), the antibacterial activity was significantly improved by 1.53- and 4.23-fold after both 6 and 8 h of culture at 93 and 89% relative inhibition, respectively, because of the hydrophilicity of poly(AA),[45] and the biological activity of the free amino groups at the C2 position of the native CS.[46] The higher antibacterial activities of the CS-*g*-poly(AA) hydrogel can be caused by the interaction between the negative charges on the bacteria surface with the positive surface of the CS-*g*-poly(AA). The more positively charged hydrogels could promote bacterial adhesion onto the hydrogel surface and reduce the remaining amount in the free suspension, resulting in a decrease in the bacteria colonies in the liquid medium. It is relevant to note here that the molar ratio amount of the AA or HEMA monomers that were grafted onto the CS is almost the same for the three different grafted CS derivatives studied here.

It was anticipated that the pores on the CS-*g*-poly(AA) hydrogel surface would improve the ability to capture bacteria. Although, the relative inhibition of the CS-*g*-poly(AA-*co*-HEMA) hydrogel

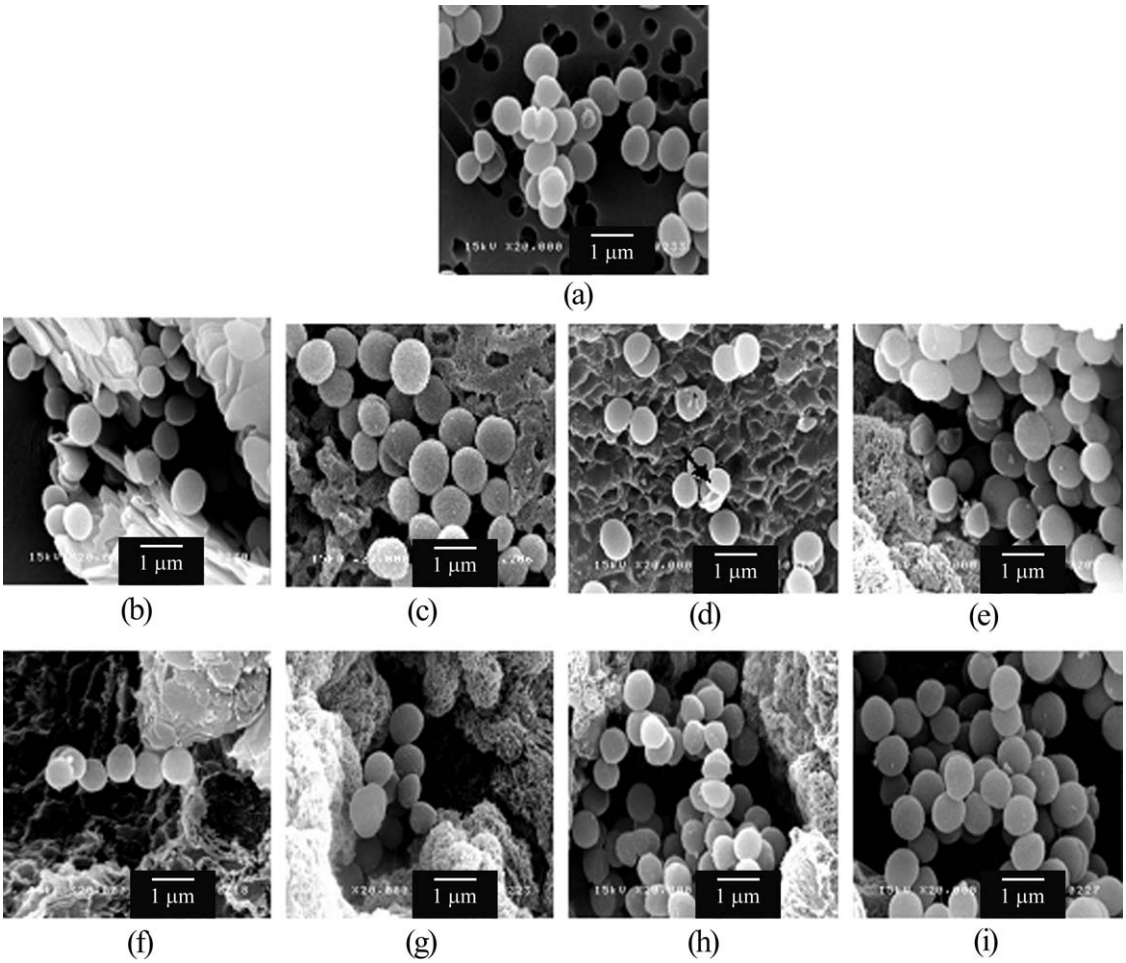

Figure 6. Representative SEM micrographs of *S. aureus* after co-culture for 24 h with (a) negative control, (b) mica, (c) CS-*g*-poly(AA), (d) CS-*g*-poly(-HEMA), (e) CS-*g*-poly(AA-*co*-PHEMA) and CS-*g*-poly(AA-*co*-PHEMA)/mica nanocomposites with mica loadings of: (f) 5%, (g) 7%, (h) 10%, and (i) 15% w w^{-1} based on the monomer. The arrow in (d) highlights a damaged cell.

would be higher than that of CS, because of the hydrophilicity resulting from the carboxyl group of poly(AA), the surface of the CS-*g*-poly(AA-*co*-HEMA) hydrogel is much rougher than the ungrafted CS hydrogel surface, which may increase bacterial adhesion sites and result in a higher antibacterial activity in the CS-*g*-poly(AA-*co*-HEMA) hydrogel than that of the CS. However, the relative inhibition of the CS-*g*-poly(AA-*co*-HEMA) hydrogel was found to actually be 1.35- and 3.3-fold lower than that of the *CS-g*-poly(AA) hydrogel in the early (6 h) and late (8 h) log phases, respectively. This is likely to be due to the decreased hydrophilicity of the HEMA moiety[45], and the relatively higher acidity of CS-*g*-poly(AA) hydrogel. Thus, graft copolymerization of CS with a 1 : 1 molar ratio of AA : HEMA can delay (or inhibit) the growth of *S. aureus* in the early exponential phase.

The antibacterial activity of the CS-*g*-poly(AA-*co*-HEMA)/mica nanocomposite hydrogels are summarized in Table III. The relative inhibition of CS-*g*-poly(AA-*co*-HEMA)/mica nanocomposite hydrogels having mica loadings at 7 and 10% w w^{-1} of the monomer was slightly higher (1.3- and 1.11-fold) at a culture time of 6 h than that of the CS and CS-*g*-poly(AA-*co*-HEMA) hydrogel, respectively. This finding is in agreement with those reported by Wang et al.[18] However, CS-*g*-poly(AA-*co*-HEMA) exhibited higher relative inhibition against *S. aureus* growth by 1.2- and 1.1-fold comparing with 10 and 7% w w^{-1} mica loading, respectively, at 8 h of culture. Increasing the mica loading to 15% w w^{-1} of the monomer significantly decreased the apparent antibacterial activity by 2.03- and 2.13-fold of that seen with no mica addition, and 2.25- and 1.9-fold of that seen with a 7% w w^{-1} mica loading after 6 and 8 h of culture, respectively. This result agreed quite well with Meng et al.,[19] finding that CS intercalated mica hydrogels could kill more bacteria than the neat CS or the clay minerals.

Nanocomposite hydrogels can generate a larger surface area to absorb more bacterial colonies and so give a greater chance to increase the antibacterial activity through interactions between the positive charges of the CS hydrogel and the negative charges on the cytoplasmic cell membrane of the bacteria.[18,46] In addition, *S. aureus* does not have an outer membrane to prevent the influx of foreign molecules[46] and so it can be inhibited more easily. However, the higher mica loading at 15% w w^{-1} of the monomer revealed a significantly decreased

level of relative inhibition of *S. aureus* growth. This might be because the higher mica content screens and prevents the polymer chains from adhering with the bacteria to trigger the antibacterial activity.

Minimum Inhibition Concentration (MIC). The MIC obtained for the CS-*g*-poly(AA) at 1.56 mg mL^{-1} against the 0.01 A_{610} units of *S. aureus* cultured in MHB for 24 h (i.e. to the late stationary phase) at room temperature was 16- and >16-fold better than those of CS and CS-*g*-poly(HEMA), respectively (Table IV). These MICs agree with that of viable counts and relative inhibition of *S. aureus* in the log phase of growth (Table III). The extent of the water absorbency and acidity of the hydrogels plays influencing roles as described in the total plate count method for the MIC result. The more the hydrogel expanded, the higher the number of colonies of *S. aureus* that could be trapped and inhibited through the diffusion effect by water in the hydrogel. The higher acidic moiety of the CS-*g*-poly(AA) hydrogels, which carry a higher positive charge, may enhance the inhibitory effect with CS. It is worth noting that the presence of the COO^- group in the poly(AA) containing hydrogels (CS-*g*-poly(AA) and CS-*g*-poly(AA-*co*-HEMA)) becomes a major driving force for bacterial adhesion in the positively charged CS. AA in the feed is a key factor governing the antibacterial property in the resulting hydrogel and nanocomposites hydrogels. The high MIC value for the CS-*g*-poly(HEMA) was potentially caused by the proposed semi-IPN structure and the rigid conformation of poly(HEMA) chains grafted onto the CS backbones.

Surprisingly, the CS-*g*-poly(AA-*co*-HEMA)/mica nanocomposite hydrogels with mica loadings of 5, 7, 10 and 15% w w^{-1} of the monomer had the same MIC values as each other and as that for the CS-*g*-poly(AA-*co*-HEMA) hydrogel (Table IV). This correlates with the almost constant water absorbency observed for the CS-*g*-poly(AA-*co*-HEMA) and the CS-*g*-poly(AA-*co*-HEMA)/mica nanocomposite hydrogels regardless of the mica loadings but relatively lower water absorbency at 15% w/w. Likewise, a much higher concentration of CS (25 mg mL^{-1}) or CS-*g*-poly(HEMA) (>25 mg mL^{-1}) or CS-*g*-poly(AA-*co*-HEMA)/mica nanocomposite hydrogels (12.5 mg mL^{-1}) is required for inhibiting *S. aureus* after 24 h of incubation.

Typical SEM micrographs of *S. aureus* cells cultured for 24 h in the MHB media alone (negative control), and in the various grafted CS copolymer and CS-*g*-poly(AA-*co*-HEMA)/mica nanocomposite hydrogels are shown in Figure 6. Since the positive control in the total plate count did not produce any viable cells, thus the positive control in MIC was not performed. The normal roundish-shapes of *S. aureus* cells were evident when cultured in the MHB media alone and also as adhered on the surface of mica [Figure 6(a–b), respectively]. However, the cell walls of some of the *S. aureus* in or on the CS-*g*-poly(HEMA) and CS-*g*-poly(AA-*co*-HEMA) hydrogels after culture for 24 h were destroyed to give open cells [Figure 6(c) as shown in Figure 6(d)]. Moreover, the *S. aureus* cells that were adsorbed and immobilized on the surface and in the pores of the CS-*g*-poly(AA-*co*-HEMA)/mica nanocomposite hydrogels, some had distorted shapes and were destroyed to give fractured cell walls and these were randomly distributed in the hydrogel matrix [Figure 6(e–h)].

Although the water absorbency of the nanocomposite hydrogels was relatively lower than that of the grafted CS hydrogel, the hydrogels had larger surface area to absorb more bacterial colonies.[18] Through this compensation, the MIC values of nanocomposite hydrogels are not different from that of the grafted CS hydrogel. Thus, CS-*g*-poly(AA-*co*-HEMA) hydrogel or CS-*g*-poly(AA-*co*-HEMA)/mica nanocomposite hydrogel was at an equilibrium condition and gave similar MIC values.

The MIC values and SEM micrographs support that the mica content in the grafted CS hydrogel did not influence the antibacterial activity. On the other hand, the different results from the plate count method are caused by the absorbance assays undertaken in the mid- and late-log phases of growth at 6 and 8 h, respectively, whilst the MIC was evaluated at a late stationary phase (24 h). The different culture times could have resulted in different cell numbers due to different chances of cell adsorption by the nanocomposite hydrogels, as well as growth and death rates

CONCLUSION

CS was used to graft with AA and/or HEMA to give the grafted-CS hydrogels. CS-*g*-poly(AA-*co*-HEMA)/mica nanocomposite hydrogels were synthesized at different mica loadings and all hydrogels were characterized by FT-IR spectroscopy, SEM, XRD, TEM and equilibrium water absorbency. FT-IR spectroscopy indicated that the CS was grafted at the NH_2 and OH sites on the CS backbone for all hydrogels and nanocomposite hydrogels. The water absorbency of the CS-*g*-poly(AA) hydrogel was the highest whilst those of CS and CS-*g*-poly(HEMA) were the lowest. The CS-*g*-poly(AA-*co*-HEMA)/mica nanocomposite hydrogels had an intercalated structure, as revealed by XRD and TEM analyses.

At the fixed 1 : 1 molar ratio of AA : HEMA, the extent of water absorbency of the nanocomposite hydrogels was constant at 5, 7 and 10% (w w^{-1} of the monomer) mica loading but slightly decreased at 15% w w^{-1} mica loading. The CS-*g*-poly(AA) hydrogel can inhibit the early-to-mid-log phase growth of *S. aureus* up to 93% with a MIC value as low as 1.56 mg mL^{-1}. For the CS-*g*-poly(AA-*co*-HEMA)/mica nanocomposite hydrogels, the relative inhibition was very similar (at ~ 81%) with mica loadings of 5, 7 and 10% w w^{-1} of the monomer, but abruptly decreased at a 15% w w^{-1} mica loading. Regardless of the mica loading levels in the CS-*g*-poly(AA-*co*-HEMA)/mica nanocomposite hydrogels, the MIC value at the late stationary phase was constant at 12.5 mg mL^{-1}. The CS-*g*-poly(HEMA) had a greater MIC (>25 mg mL^{-1}) than CS (25 mg mL^{-1}). Several possible explanations for the different inhibitory activities against *S. aureus* are discussed, but some are awaiting further research for clarification.

ACKNOWLEDGMENTS

The authors would like to acknowledge the financial support from the Thailand Research Fund under the Research Team Aided Program Contract no. RTA5080004. Partial financial support from the

Graduate School, Chulalongkorn University is acknowledged. The provision of research facilities by the Imaging Polymer Laboratory of Chulalongkorn University's Department of Imaging and Printing Technology, Faculty of Science is highly appreciated. English edition by the Publication Counselor Unit of the Research Division, Faculty of Science, Chulalongkorn University, and fruitful suggestion provided by Dr. Robert Butcher are highly appreciated.

REFERENCES

1. Devine, D. M.; Higginbotham, C. L. *Eur. Polym. J.* **2005,** *41*, 1272.
2. Jung, J. J; Youn, D. K.; Lee, S. H.; No, H. K.; Ha, J. G.; Prinyawiwatkul, W. *Int. J. Food. Sci. Technol.* **2010,** *45*, 676.
3. Wang, J.; Lian, Z.; Wang, H.; Jin, X.; Liu, Y. *J. Appl. Polym. Sci.* **2012**, *123*, 3242.
4. Rinaudo, M. *Prog. Polym. Sci.* **2006,** *31*, 603.
5. Dos Santos, K. S. C. R.; Coelho, J. F. J.; Ferreira, P.; Pinto, I.; Lorenzetti, S. G., Ferreira, E. I.; Higa, O. Z.; Gil, M. H. *Int. J. Pharm.* **2006,** *310*, 37.
6. Mahdavinia, G. R.; Pourjavadi, A.; Hosseinzadeh, H.; Zohuriaan, M. J. *Eur. Polym. J.* **2004,** *40*, 1399.
7. Jalal Zohuriaan-Mehr, M. *Iran. Polym. J.* **2005,** *14*, 235.
8. Carenza, M. *Int. J. Radiat. Appl. Instrum. C. Radiat. Phys. Chem.* **1992,** *39*, 485.
9. Schweikl, H.; Hartmann, A.; Hiller, K. -A.; Spagnuolo, G.; Bolay, C.; Brockhoff, G.; Schmalz, G. *Dent. Mater.* **2007,** *23*, 688.
10. Pawlowska, E.; Poplawski, T.; Ksiazek, D.; Szczepanska, J., Blasiak, J. *Mutat. Res.* **2010,** *696*, 122.
11. Tanodekaew, S.; Prasitsilp, M.; Swasdison, S.; Thavornyutikarn, B.; Pothsree, T.; Pateepasen, R. *Biomaterials* **2004,** *25*, 1453.
12. Sahu, K.; Verma, Y.; Sharma, M.; Rao, K. D.; Gupta, P. K. *Skin Res Technol* **2010,** *16*, 428.
13. Tang, C.; Chen, N.; Zhang, Q.; Wang, K.; Fu, Q.; Zhang, X. *Polym. Degrad. Stabil.* **2009,** *94*, 124.
14. Wang, X.; Du, Y.; Luo, J.; Yang, J.; Wang, X.; Shi, X.; Hu, Y. *Polymer* **2006,** *47*, 6738.
15. Wang, X.; Du, Y.; Luo, J.; Yang, J.; Wang, W.; Kennedy, J. F. *Carbohydr. Polym.* **2009,** *77*, 449.
16. Xie, Y.; Wang, A.; Liu, G. *Polym. Compos.* **2010,** *3*, 89.
17. Wang, X.; Du, Y.; Yang, J.; Tang, Y.; Luo, J. J. *J. Biomed. Mater. Res.* **2008**, *84A*, 384.
18. Wang, X.; Du, Y.; Luo, J.; Lin, B.; Kennedy, J. F. *Carbohydr. Polym.* **2007,** *69*, 41.
19. Meng, N.; Zhou, N.; Zhang, S.; Shen, J. *Appl. Clay. Sci.* **2009,** *42*, 667.
20. Bozhilov, K. N.; Xu, Z.; Dobrzhinetskaya, L. F.; Jin, Z. -M.; Green, H. W., II. *Lithos* **2009,** *109*, 304.
21. Tjong, S. C. Synthesis and Structure-Property Characteristics of Clay-Polymer Nanocomposites, Nanocrystalline Materials; Elsevier: Oxford, **2006;** Chapter 10, p 311.
22. Hsu, S.; Tseng, H.; Hung, H.; Wang, M.; Hung, C.; Li, P.; Lin, J. *Appl. Mater. Interface.* **2009,** *11*, 2556.
23. Li, P.; Wei, J.; Chiu, Y.; Su, H.; Peng, F.; Lin, J. *Appl. Mater. Interface.* **2010,** *2*, 1608.
24. Patil, D. R., Fanta, G. F. *J. Appl. Polym. Sci.* **1993,** *47*, 1765.
25. Lanthong, P.; Nuisin, R.; Kiatkamjornwong, S. *Carbohydr. Polym.* **2006,** *66*, 229.
26. Mun, G. A.; Nurkeeva, Z. S.; Dergunov, S. A.; Nama, I. K.; Maimakov, T. P.; Shaikhutdinov, E. M.; Lee, S. C.; Park, K. *React. Funct. Polym.* **2008,** *68*, 389.
27. Sun, T.; Zhou, D.; Xie, J.; Mao, F. *Eur. Food. Res. Technol.* **2007,** *225*, 451.
28. Zhang, J.; Wang, Q.; Wang, A. *Carbohydr. Polym.* **2007,** *68*, 367.
29. Singha, V.; Sharmaa, A. K.; Tripathi, D. N.; Sanghib, R. *J. Hazard. Mater.* **2009,** *161*, 955.
30. Huacai, G.; Wan, P.; Dengke, L. *Carbohydr. Polym.* **2006,** *66*, 372.
31. Mishra, D. K.; Tripathy, J.; Srivastava, A.; Mishra, M. M.; Behari, K. *Carbohydr. Polym.* **2008,** *74*, 632.
32. Casimiroa, M. H.; Botelho, M. L.; Leal, J. P.; Gil, M. H. *Radiat. Phys. Chem.* **2005,** *72*, 731.
33. Semenzato, S.; Lorenzetti, A.; Modesti, M.; Ugel, E.; Hrelja, D.; Besco, S.; Michelin, R. A.; Sassi, A.; Facchin, G.; Zorzi, F.; Bertani, R. *Appl. Clay. Sci.* **2009,** *44*, 35.
34. Dai, H.; Li, H.; Wang, F. *Surf. Coat. Technol.* **2006,** *201*, 2859.
35. Bayramoğlu, G.; Arica, M. Y. *Colloids. Surf. A.* **2002,** *202*, 41.
36. Wang, J. P.; Chen, Y. Z.; Zhang, S. J.; Yu, H. Q. *Bioresour. Technol.* **2008,** *99*, 3397.
37. Luckachan, G. E.; Pillai, C. K. S. *Carbohydr. Polym.* **2006,** *64*, 254.
38. Kittur, F. S.; Kumar, A. B. V.; Tharanathan, R. N. *Carbohydr. Res.* **2003,** *338*, 1283.
39. Krishna Rao, K. S. V.; Chung, I.; Ha, C. S. *React. Funct. Polym.* **2008,** *68*, 943.
40. Sivudu, K. S.; Thomas, S.; Shailaja, D. *Appl. Clay. Sci.* **2007,** *37*, 185.
41. Sperling, L. H. Introduction to Physical Polymer Sciences, 4th ed.; John Wiley & Sons: New York, **2006;** p 477.
42. Zhou, Y.; Yang, D.; Gao, X.; Chen, X.; Xu, Q.; Lu, F.; Nie, J. *Carbohydr. Polym.* **2009,** *75*, 293.
43. Kiatkamjornwong, S.; Mongkolsawat, K.; Sonsuk, M. *Polymer* **2002,** *43*, 3915.
44. Mohan, Y. M.; Lee, K.; Premkumar, T.; Geckeler, K. E. *Polymer* **2007,** *48*, 158.
45. Oh, S. T.; Han, S. H.; Ha, C. S.; Cho, W. J. *J. Appl. Polym. Sci.* **1996,** *59*, 1871.
46. Je, J.; Kim, S. *J. Agric. Food Chem.* **2006,** *54*, 6629.